



Contents lists available at ScienceDirect

## Biochimica et Biophysica Acta

journal homepage: [www.elsevier.com/locate/bbamem](http://www.elsevier.com/locate/bbamem)

# Impact of the biofilm mode of growth on the inner membrane phospholipid composition and lipid domains in *Pseudomonas aeruginosa*

Hayette Benamara, Christophe Rihouey, Thierry Jouenne, Stéphane Alexandre \*

PBS laboratory, UMR 6270, FR 3038, CNRS, Proteomic Platform of the IFRMP23, University of Rouen, 76821 Mont-Saint-Aignan cedex, France

## ARTICLE INFO

### Article history:

Received 2 April 2010

Received in revised form 2 September 2010

Accepted 3 September 2010

Available online 16 September 2010

### Keywords:

Biofilm

*Pseudomonas aeruginosa*

Lipidome

Inner membrane

Monolayer

Mass spectrometry

## ABSTRACT

Many studies using genetic and proteomic approaches have revealed phenotypic differences between planktonic and sessile bacteria but the mechanisms of biofilm formation and the switch between the two growth modes are not well understood yet. In this study, we focused on inner membrane lipidome modifications when *Pseudomonas aeruginosa* cells were grown as biofilm. Lipid analyses were performed by Electrospray Ionization Mass Spectrometry. Results showed a drastic decrease of the uneven-numbered chain phospholipids and a slight increase of long chain PEs in sessile organisms as compared with planktonic counterparts, suggesting a better lipid stability in the bilayer and a decrease in membrane fluidity. The impact of sessile growth on lipid domains was then investigated by Brewster Angle Microscopy (BAM) and Atomic Force Microscopy (AFM). Observations showed that inner membrane lipids of *P. aeruginosa* formed domains when the pressure was close to physiological conditions and that these domains were larger for lipids extracted from biofilm bacteria. This is coherent with the mass spectrometry analyses.

© 2010 Elsevier B.V. All rights reserved.

## 1. Introduction

It is now accepted that microbial populations use cell attachment to solid supports to survive, forming structured communities called biofilms. A bacterial biofilm may be described as a structured community of bacteria enclosed in a self-produced polymer matrix and adherent to inert or living surface [1]. Biofilms are universal [2] and far more resistant to antimicrobial agents than planktonic bacteria [1,3,4]. This increased resistance of bacterial biofilm to antibiotics is a crucial problem for the treatment of persistent and chronic infections. Despite this definite importance of the sessile state in microbial way of life and its consequences for human beings, our present knowledge of the physiology of sessile bacteria still remains fragmentary [5]. Consequently, it is of great importance to understand the causal basis of biofilm formation and biofilm traits.

Three major mechanisms have been proposed to account for the increased resistance of biofilms to antimicrobial agents [6]. The first hypothesis relates to the polymer matrix which prevents inhibitors from reaching cellular targets. However, some studies suggested that the role of the exopolymer matrix is limited and dependent of the class of antibiotics [7,8]. The second hypothesis is that cells in the deeper layer of thick biofilms, which grow more slowly, have less access to nutrient and then to antibiotics. Several authors provided evidence in support of the second theory of biofilm resistance, whether by controlling the growth rate of bacteria through nutrient

limitation [9] or by comparing the resistance to antimicrobial agents between young and mature biofilms [10]. The third hypothesis assumes the existence of a “biofilm phenotype”. In support of this hypothesis, it has been found that antibiotic-resistant phenotypic variants of *Pseudomonas aeruginosa* with enhanced ability to form biofilms arise at high frequency both in vitro and in the lungs of CF patients. It has also been shown that there is a regulatory protein (PvrR) which controls the conversion between antibiotic-resistant and antibiotic-susceptible forms [11].

Differentiation in biofilm development has thus been explored in increasing details since the 80s. Thus, a great number of genetic [12–16] and proteomic investigations [17–20] have been devoted to determine the degree to which gene regulation during biofilm development controls the switch from planktonic to biofilm growth. While most protein-based approaches suggest that many genes are differentially regulated during biofilm development – confirming significant physiological differences between free-living and biofilm bacteria [21] – transcriptome analyses led to the conclusion that only 1% (i.e., 73 genes) of *P. aeruginosa* genes showed differential expression in planktonic and biofilm cells [16].

*P. aeruginosa* is a common opportunistic and nosocomial pathogen and the leading cause of morbidity and mortality in cystic fibrosis patients [22]. *P. aeruginosa* biofilms are involved in the pathogenesis of urinary, ventilator-associated pneumonia, peritoneal dialysis catheter infections, bacterial keratitis, otitis externa and burn wound infections [1]. For these reasons, *P. aeruginosa* biofilm is one of the most widely studied biofilm models.

In 2004, a proteomic study revealed that sessile *P. aeruginosa* cells accumulated some enzymes (e.g., the acetyl-CoA acetyl transferase

\* Corresponding author. Tel.: +33 235 14 67 80; fax: +33 235 14 67 09.

E-mail address: [stephane.alexandre@univ-rouen.fr](mailto:stephane.alexandre@univ-rouen.fr) (S. Alexandre).

(ato B) and the probable short-chain dehydrogenase) which are involved for fatty acid and phospholipids biosynthesis [20]. Among proteins accumulated by *P. aeruginosa* when grown in biofilm, were the acylase and B-hydroxydecanoyl-acyl carrier protein (ACP) [18]. These data question about the impact of the sessile growth state on the bacterial lipid content, i.e. the lipidome.

The aim of the present work was to characterize eventual changes in phospholipid composition between planktonic and sessile *P. aeruginosa* cells. Lipid analyses were carried out by Electrospray Ionization Mass Spectrometry (ESI-MS). The impact of the biofilm growth mode on phospholipid organisation has also been studied by reconstitution in monolayer membrane models and thus visualization by Brewster Angle Microscopy (BAM) and Atomic Force Microscopy (AFM).

## 2. Material and methods

### 2.1. Bacterial strain and preculture

*P. aeruginosa* PAO1 strain was used. Bacteria were stocked in Muller-Hinton broth (MHB) with 30% (v/v) glycerol. Preculture was performed in 50 mL flask containing 1 mL of bacterial stock suspensions and 10 mL of MHB. The flask was incubated at 37 °C on a rotary shaker (140 rpm) for 18 h.

### 2.2. Planktonic cultures

After incubation, the preculture was used to inoculate 100 mL of Minimal Glucose Medium MGM (15 g/L Tris-HCl, 0.6 g/L Tris-base, 0.5 g/L NH<sub>4</sub>Cl, 2 g/L yeast extract, 0.05 g/L CaCl<sub>2</sub>, 0.05 g/L MgSO<sub>4</sub>, 0.005 g/L FeSO<sub>4</sub>, 0.005 g/L MnSO<sub>4</sub>, and 15 g/L glucose) at a final concentration of 10<sup>7</sup> Colony Forming Units (CFU)/mL. Three cultures of 100 mL MGM were simultaneously carried out in 250 mL Erlenmeyer flasks and were incubated on a rotary shaker (140 rpm) at 37 °C for 24 h.

### 2.3. Biofilm formation

One hundred milliliters of MGM containing 2 g (total surface area 2800 cm<sup>2</sup>) of sterile glass wool (Merck®) was inoculated at 10<sup>7</sup> CFU/mL from a preculture, as previously described [16]. Cells were grown under slight agitation (10 rpm) at 37 °C for 24 h.

### 2.4. Bacteria recovery from biofilm

Glass wool was aseptically removed and washed twice in 0.1 M, pH 7 Phosphate Buffer Saline (PBS) to release weakly attached cells. It was then placed in sterile flasks containing 30 g of glass beads (diameter, 3 mm) and 50 mL of PBS. Biofilm organisms were released from the substratum by vigorous shaking for 20 min.

### 2.5. Inner membrane extractions

Bacterial inner membrane extraction was carried out following the spheroplast protocol first described by Mizuno and Kageyama [23]. Briefly, bacteria (planktonic or sessile cells) were harvested at 4 °C for 10 min at 2600 ×g and washed in 10 mL of 20% (w/v) sucrose. Pellets were weighted and then resuspended in a digestion solution of the following composition: for 1.5 g bacteria wet weight, 18 mL of 20% sucrose, 9 mL of 2 M saccharose, 10 mL of 0.1 M Tris-HCl, 0.8 mL of 1% EDTA, 1.8 mL of 1% lysozyme, 1 μL of 1 mg/mL RNase and 5 μL of 20 mg/mL DNase. The solution was incubated at 37 °C. Spheroplast formation was monitored by optical microscopy. When only ovoid forms were observed, the suspension was centrifuged at 30 °C for 15 min at 5200 ×g to recover spheroplasts. The pellet was resuspended in 5 mL of 0.01 M PBS and was subjected to sonication (cycles of 30 s for 2 min). The suspension was then centrifuged at 30 °C, for 20 min at 5200 ×g. The supernatant, containing inner membrane, was

diluted in 100 mM sodium carbonate, stirred at 4 °C for 1 h to separate soluble and insoluble phase and then was ultracentrifuged (60,000 ×g for 1 h at 4 °C) to harvest inner membrane. Pellets were washed twice with 40 mM Tris buffer (pH 7) and freeze-dried at −20 °C.

### 2.6. Extraction of inner membrane lipids

Lipid extraction was carried out according to Bligh and Dyer protocol [24]. For 1 mL of membrane extract, 3.75 mL of chloroform:methanol (1:2 v/v) solution was added. The mixture was sonicated for 5 min and vortexed for 15 min until obtaining a milky-mixture. After adding 1.25 mL of chloroform, the mixture was vortexed for 1 min. A volume of 1.25 mL of 1 M NaCl aqueous solution was added and the mixture was vortexed again for 15 min. Finally, the mixture was centrifuged (670 ×g for 10 min at 30 °C) to separate organic and aqueous phase. The organic phase was recovered with a Pasteur pipette and 1.88 mL of chloroform was added to the aqueous phase. After stirring for 15 min, the mixture was centrifuged (670 ×g for 10 min at 30 °C) to separate the two phases. The aqueous phase was removed and organic phases were mixed and evaporated under argon.

To eliminate proteolipids, 1 mL of methanol was added to lipid extracts. The mixture was vortexed to degrade proteins. Methanol was then evaporated. A chloroform:methanol (1:2 v/v) solution was added and the mixture was centrifuged (670 ×g for 10 min at 30 °C), to sediment proteins. The organic phase was recovered and evaporated under argon. The lipid extract was conserved at −20 °C.

### 2.7. Lipid extracts analysis

Mass spectral analyses were performed by Electrospray Ionization Mass Spectrometry (ESI-MS). ESI-MS allows the formation of gaseous ions from polar, thermally labile and mostly non-volatile molecules and thus is completely suitable for phospholipids [25]. It is a method of measuring m/z ratios of individual and ionized molecules and their fragmentation products.

The spectrometer used is a Linear Quadrupole Ion Trap (QTRAP®, AB Sciex Instruments™) equipped with a turbo spray ionization source heated to 300 °C. The potential applied during the acquisition was −3500 V. The mass calibration and resolution were made according to the procedure of the manufacturer's specifications.

The stock solution of lipid extracts was then diluted at a concentration of 1 μmol (see Brewster Angle Microscopy section). The solution was subjected to sonication for 1 h to obtain stable and homogeneous solution. Samples were infused at 10 μL/min flow rate in negative ionization mode. Spectra were acquired at 1000 amu s<sup>−1</sup> over the 50–1700 m/z range.

Spectra were analysed via a home-made Python script under the free scientific data analysis software SciDAvis (<http://scidavis.sourceforge.net/>). In each case (planktonic and sessile bacteria), three spectra from lipid extracts were analysed. Analysis of variance (ANOVA) was then performed to see if the increase or decrease of the peak is statistically relevant or not. The p-value was calculated using the script from Pr. Hossein Arsham (<http://home.ubalt.edu/ntsbarsh/Business-stat/otherapplets/pvalues.htm>).

### 2.8. Characterization of lipids after reconstitution in monolayer

#### 2.8.1. Brewster Angle Microscopy

BAM allows *in situ* studies of thin films at air/water interfaces. This technique allows the observation of lipid domains without using a fluorescent probe.

The microscope used is a BAM 2+ (NFT, Germany) with 2 μm resolution. The home-made trough used is made of non-porous Teflon. This trough measures 27 cm long and 7.5 cm wide for a volume of 200 mL, and is equipped with a Teflon barrier at each extremity. The trough is equipped with a Wilhelmy balance (R&K, Germany) for

measuring surface pressure. It was cleaned with a sodium octanoate solution (1 g/L) and rinsed several times with milli-Q water.

Lipid extracts were diluted in a chloroform:methanol (80:20 v/v) solution. The volume of solvent was adjusted in order to obtain a 1 mM stock solution. To elaborate a monolayer at the air/water interface, a volume of 45  $\mu$ L of lipid solution was spread at the water surface with a micropipette. After evaporation of the solvent during 15 min, surface pressure was increased by moving the two barriers through the middle of the trough. The concentration of the stock solution was checked by plotting a pressure–area isotherm which was compared to an isotherm of a phospholipid reference solution.

Images were taken at different surface pressures ranging from 0.2 to 35 mN/m in order to monitor the evolution of the lipid monolayer. In each case (planktonic and sessile bacteria), two lipid extracts were visualized. Domain diameters were evaluated from 2 different images for each sample for monolayers at 30 mN/m (581 domains for planktonic bacterial lipid extracts and 297 domains for sessile bacterial lipid extracts). ANOVA was performed using a Python script in SciDAVis software to see how statistically relevant are the differences observed.

### 2.8.2. Atomic Force Microscopy

Lipid monolayer was transferred onto a muscovite plate and then placed in a desiccator cabinet for at least 24 h. The transfer was carried out using the technique of Langmuir–Schaeffer, which is dipping a

support through the hydrophilic film and lifting it back horizontally. The transfer was carried out at a surface pressure of 30 mN/m. Observations were performed by using a Nanoscope III Multimode microscope (Veeco, Santa Barbara, CA) with a 100  $\mu$ m piezoelectric scanner. All measurements were achieved in the air in the contact mode. The cantilevers used were characterized by a low spring constant of about 0.06 N/m. All the measurements were performed with the feedback loop on (constant force from 10–9 to 10–8 N). No processing was used on images except for a flatten operation. All images are presented in the height mode (color palette for height: dark colors for low zones, light colors for high zones) and are top-view images.

## 3. Results

### 3.1. Mass spectrometry analysis of lipid extracts

The phospholipid composition of *P. aeruginosa* inner membrane was characterized by the predominance of phosphatidylethanolamines (PEs) and phosphatidylglycerols (PGs) in both planktonic and sessile cells (Fig. 1). Both exhibited a preponderant ion at 716.6 which corresponds to PE 34:1. Only few chlorinated phosphatidylcholine PCs were detected. Phosphatidic acids (PAs) were also present in the lower masses, although they might be due to phospholipid fragmentation. The comparison of MS spectra of lipids extracted from planktonic and sessile bacteria showed that phospholipids with an

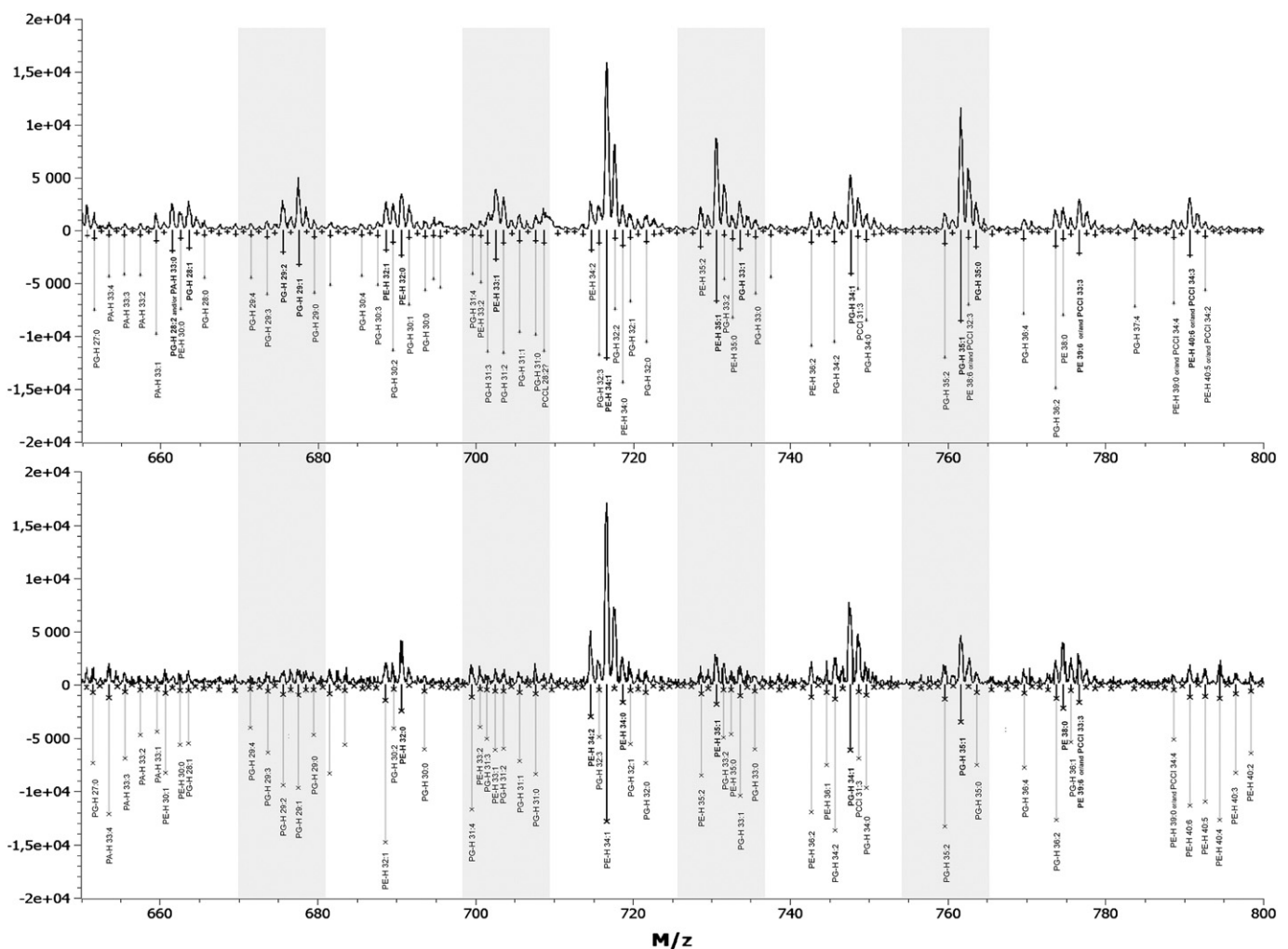


**Fig. 1.** Mass spectra of lipid extracts and identification of phospholipids: (top) lipid extracts from planktonic bacteria; (bottom) lipid extracts from sessile bacteria. Below identified peaks a bar (in negative value) gives the corrected intensity of the peak. This corrected intensity takes into account the intensity of the +1 isotopic mass value of the identified preceding lipid. Intensities of the lowest peaks have been multiplied by 10 and are featured as grey bars. The region corresponding to uneven-numbered chains has been enlightened in grey.

uneven number of carbon atoms (uneven-numbered chains) were drastically depressed when bacteria were grown in biofilm (Fig. 1, enlightened zones in grey). An examination of the lipids with even-numbered chains also revealed a slight increase of PEs with longer chains (PE 36 to PE 40). The predominant PE ions in planktonic bacteria were (in order of importance) PE 34:1, PE 35:1, PE 33:1, PE 32:0, PE 34:2 and PE 32:1 while in sessile bacteria they were PE 34:1, PE 34:2, PE 32:0, PE 38:0, PE 35:1 and PE 34:0. For PGs, in planktonic bacteria they were PG 35:1, PG 34:1, PG29:1, PG 29:2, PG 33:1 and PG 35:0, and in sessile bacteria PG 34:1, PG 35:1, PG 34:2, PG 35:2, PG 36:2 and PG 31:4. The evolution of the phospholipids is summarized in Table 1. From the predominant ions, the most increased peaks in sessile bacteria corresponded to PE 34:2 (by a factor of 2.6) and PG 34:1 (factor of 1.5) while the most diminished peaks corresponded to PE 33:1, PE 35:1 and PG 29:1 (factor of 0.4) and PG 35:1 (0.5). Several low intensity ions like PG 28:0, PG 32:0, PG 34:i, PE 36:i, PG 36:i, PE 38:i and PE 40:i are also found to have a statistically relevant increase. Low intensity peaks attributed to PCs are also found to statistically decrease. However this has to be taken with caution since PCs are detected with a low intensity. It should be noticed that all statistically relevant increased peaks corresponded to even-numbered chains while most diminished peaks corresponded to uneven-numbered chains (excepted for PG 28:1 and PCs).

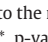
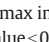
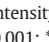

### 3.2. Brewster Angle Microscopy

Images taken at low surface pressures (0.2 mN/m) were characteristic of transition between gas phase (lack of reflection: black) and

liquid expanded phase (low reflection: medium grey) in both planktonic and biofilm growth mode (Fig. 2A1 and B1). The gas phase corresponds to free phospholipids in the monolayers and only happens at very low surface pressure when lipids are not tightly packed. To get a phospholipid organisation similar to that in biological membrane (corresponding to mixture of liquid expanded, liquid condensed and eventually solid domains), the lipids have to be packed (compressed) leading to an increase in surface pressure [26]. When the surface pressure was increased by compression of the monolayer, the gas phase disappeared and the monolayer was then in a liquid expanded phase (Fig. 2A2 and B2). In this phase, the lipids are quite free to move but the lateral diffusion of phospholipids is limited. Aggregates exhibiting a higher reflection were also observed (white objects). The number of aggregates per area unit increased steadily during compression. Circular condensed phase domains (light grey spots) began to appear spontaneously from 15 to 20 mN/m for both planktonic and biofilm organisms (Fig. 2A3, A4, B3, B4). Condensed domains around the aggregates are also observed. In these condensed domains, the phospholipids are packed tightly, their tails are free to rotate but exhibit the same angle to the normal. Lateral diffusion is highly limited. These condensed domains were surrounded by liquid expanded phase.

The diameters of the spontaneously formed domains were measured and the results are shown in Fig. 3. Actually in the case of the lipid extracts from the biofilms, two size distributions are observed. In the case of the lipid extracts from planktonic bacteria, the smallest size distribution is impossible to observe with the BAM and has been confirmed from AFM images (left part of the figure). It is

**Table 1**

Intensity alteration of identified lipids in planktonic and sessile bacteria. This is compiled from three spectra for each planktonic and sessile bacterial lipid extracts. Intensity level compared to the max intensity:  >40%;  >20%;  >10%;  <10%. Uneven-numbered chain phospholipids are highlighted in grey. Results of the ANOVA are shown in the F-test column: \*\*\*, p-value < 0.001; \*\*, p-value < 0.01; \*, p-value < 0.05; +, p-value < 0.1; none, p-value > 0.1 (not statistically relevant). Lipids corresponding to the most prominent peaks and with greater statistically relevant changes are typed in bold. Ratios corresponding to an increase are straight while those corresponding to a decrease are in italics.

M/z	Lipid	[1]Evolution[2] [1]⇒[2]	Intensity ratio [2]/[1]	F-test	M/z	Lipid	[1]Evolution[2] [1]⇒[2]	Intensity ratio [2]/[1]	F-test	M/z	Lipid	[1]Evolution[2] [1]⇒[2]	Intensity ratio [2]/[1]	F-test
651.5	PG-H 27:0		0.77 ± 0.49		703.46	PG-H 31:2		0.78 ± 0.9		759.5	PG-H 35:2		1.63 ± 0.92	
653.42	PA 33:4		1.80 ± 1.04		704.48	PE-H 33:0		1.33 ± 0.73		761.6	<b>PG-H 35:1</b>		<b>0.54 ± 0.15</b>	**
655.34	PA 33:3		1.38 ± 1.12		705.44	PG-H 31:1		1.36 ± 0.71		762.56	PCCl 32:3		0.32 ± 0.25	+
657.32	PA 33:2		1.51 ± 0.79	+	707.54	PG-H 31:0		0.92 ± 0.6		763.52	PG-H 35:0		0.59 ± 0.08	***
659.36	PA 33:1		0.66 ± 0.54		708.56	PCCl 28:2?		0.44 ± 0.29	+	769.52	PG-H 36:4		1.33 ± 0.3	*
661.4	PA 33:0 / PG 28:2		0.41 ± 0.42		714.56	<b>PE-H 34:2</b>		<b>2.64 ± 1.1</b>	**	771.44	PG-H 36:3		1.95 ± 0.78	*
662.48	PE-H 30:0		0.89 ± 0.36		715.58	PG-H 32:3		0.62 ± 0.43		772.52	PE-H 38:1		3.96 ± 2.42	**
663.56	PG-H 28:1		0.39 ± 0.19	*	716.54	PE-H 34:1		1.11 ± 0.22		773.6	PG-H 36:2		1.02 ± 0.39	
665.48	PG-H 28:0		1.21 ± 0.13	*	717.56	PG-H 32:2		1.09 ± 1.6		774.56	PE-H 38:0		1.58 ± 1.16	
671.42	PG-H 29:4		1.44 ± 0.93		718.58	PE-H 34:0		1.17 ± 0.4		775.52	PG-H 36:1		1.41 ± 0.99	
673.4	PG-H 29:3		1.99 ± 1.66		719.48	PG-H 32:1		1.23 ± 0.93		776.6	PCCl 33:3		0.66 ± 0.31	+
675.44	PG-H 29:2		0.46 ± 0.39	+	721.52	PG-H 32:0		2.43 ± 2.0	+	783.61	PG-H 37:4		1.00 ± 0.46	
677.48	<b>PG-H 29:1</b>		<b>0.44 ± 0.13</b>	**	728.54	PE-H 35:2		0.91 ± 0.49		785.47	PG-H 37:3		1.14 ± 0.72	
679.4	PG-H 29:0		0.80 ± 0.38		730.58	<b>PE-H 35:1</b>		<b>0.43 ± 0.17</b>	**	787.57	PG-H 37:2		2.21 ± 1.76	
685.4	PG-H 30:4		1.17 ± 0.76		731.54	PG-H 33:2		0.94 ± 0.86		788.53	PE-H 39:0		0.68 ± 0.23	+
687.5	PG-H 30:3		1.04 ± 0.68		732.56	PE-H 35:0		0.76 ± 0.24	+	790.57	PE 40:6 / PCCl 34:3		0.37 ± 0.21	**
688.52	PE-H 32:1		1.23 ± 0.55		733.52	PG-H 33:1		0.79 ± 0.29		792.55	PE-H 40:5		1.28 ± 1.27	
689.42	PG-H 30:2		0.56 ± 0.51		735.5	PG-H 33:0		1.12 ± 0.27		794.47	PE-H 40:4		3.11 ± 3.56	
690.5	PE-H 32:0		1.21 ± 0.41		742.58	PE-H 36:2		1.50 ± 0.42	*	796.57	PE-H 40:3		2.68 ± 0.3	***
691.46	PG-H 30:1		0.44 ± 0.63		744.56	PE-H 36:1		2.76 ± 1.2	**	798.49	PE-H 40:2		5.34 ± 5.65	+
693.5	PG-H 30:0		1.24 ± 0.97		745.52	PG-H 34:2		1.66 ± 0.61	*	800.53	PE-H 40:1		4.35 ± 3.83	*
699.5	PG-H 31:4		1.66 ± 1.54		746.42	PE-H 36:0		2.15 ± 1.12	**					
700.58	PE-H 33:2		1.23 ± 0.48		747.56	<b>PG-H 34:1</b>		<b>1.56 ± 0.35</b>	**					
701.72	PG-H 31:3		0.47 ± 0.55		748.52	PCCl 31:3 / PE 37:6		1.14 ± 0.72						
702.5	<b>PE-H 33:1</b>		<b>0.37 ± 0.2</b>	**	749.54	PG-H 34:0		1.35 ± 0.11	***					

[1] Intensity level of lipids from planktonic bacteria.

[2] Intensity level of lipids from sessile bacteria.

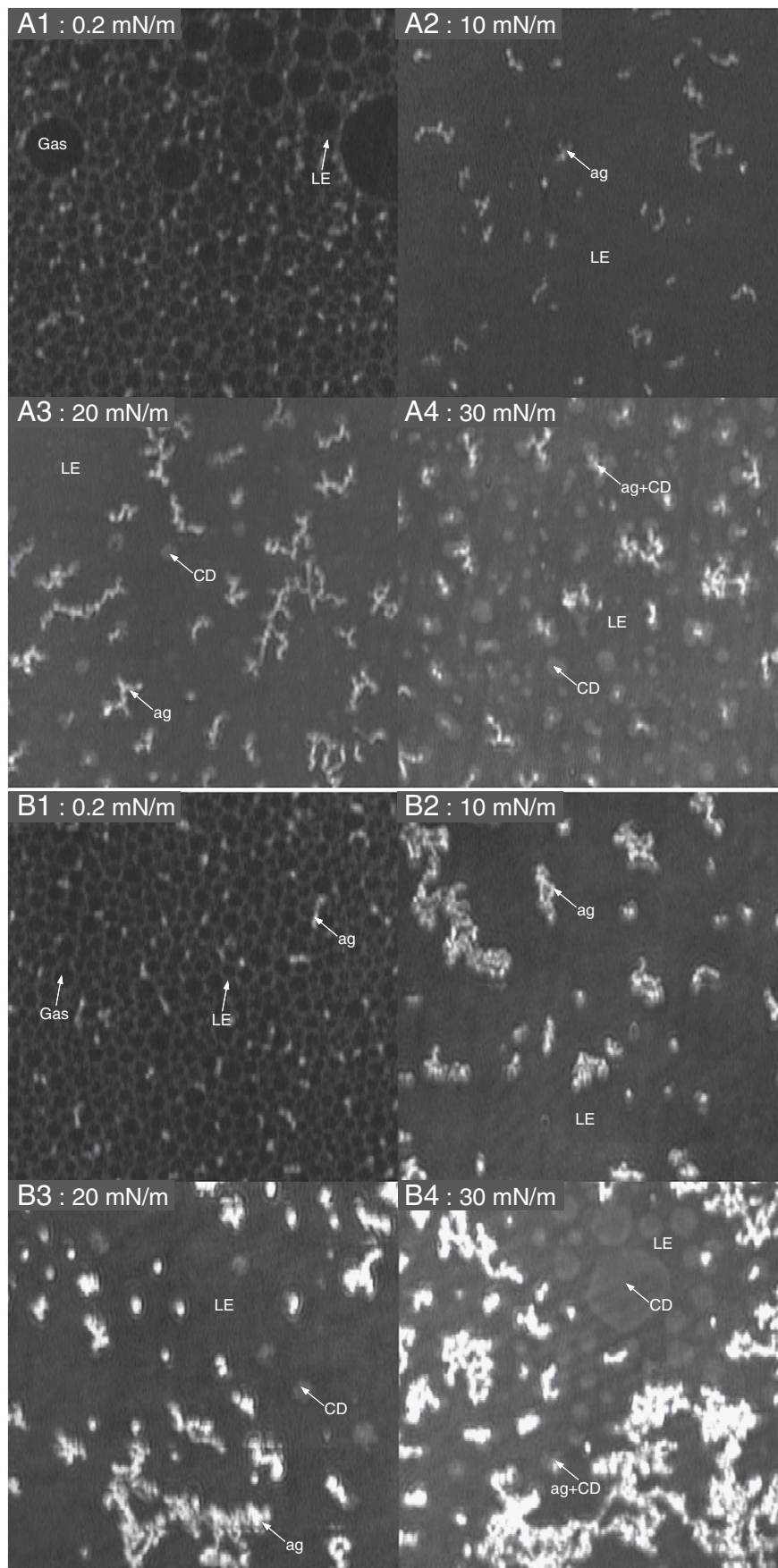


**Fig. 2.** Brewster Angle Microscopy images of lipid extract: reconstituted monolayer from A) planktonic bacteria; B) sessile bacteria. Images are  $200\ \mu\text{m} \times 200\ \mu\text{m}$ . A1) and B1) images taken at low surface pressure; Monolayers are in the transition between a gas phase and a liquid expanded phase. A2) and B2)  $\pi = 10\ \text{mN/m}$ ; The monolayers are in the expanded phase; Aggregates (white objects) are also observable. A3) and B3)  $\pi = 20\ \text{mN/m}$ ; Note the apparition of liquid condensed domains (light grey circular objects) surrounding the liquid expanded phase. A4) and B4)  $\pi = 30\ \text{mN/m}$ . Gas: gas phase; LE: liquid expanded phase; ag: aggregates; CD: condensed domain; ag + CD: condensed domain formed around an aggregate.

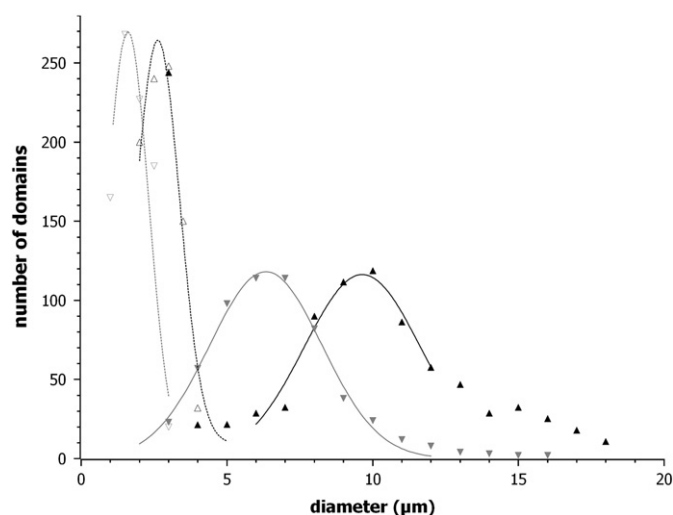


**Fig. 3.** Domains size distribution as found from the BAM images:  $\nabla$  domains from planktonic lipid extracts,  $\blacktriangle$  domains from sessile extracts. Curves were obtained by a Gaussian fit. The p-value from the ANOVA is below 0.001.  $\nabla$  and  $\triangle$  are evaluated from the AFM images since domains of diameters below 2 to 3  $\mu\text{m}$  diameters are not easily detected on the BAM images. Only in the case of the BAM images from sessile lipid extracts, small domains of 3  $\mu\text{m}$  diameters are really visible and in this case the two size distributions are clear from the BAM image.

then clear that two size distributions exist for each lipid extracts. The larger domains are found to have an average diameter of  $6.3 \pm 3.7 \mu\text{m}$  for planktonic lipid extracts and  $9.6 \pm 3.9 \mu\text{m}$  for biofilm lipid extracts. The ANOVA performed on these results give a p-value for the Fisher-test below 0.001. Therefore the difference in mean domain diameters is highly significant. Some very big domains (30 to 45  $\mu\text{m}$  diameters) were also observed with the biofilm lipid extract monolayer.

### 3.3. Atomic force microscope observations

AFM images confirmed the molecular organisations previously observed by BAM. The film obtained with lipids purified from both planktonic and sessile bacteria, exhibited circular domains of condensed phases surrounded by a continuous liquid expanded phase (Fig. 4). Condensed domains formed around the aggregates were also observed. The height difference between the condensed circular domains and the surrounding expanded phase was low (0.6 nm) and mainly due to differences in the state of lipid condensation: the aliphatic chains of lipids in condensed domains

were adjusted along an axis almost vertical, while phospholipids in liquid expanded phase were 2 to 3 times less dense, implying lower average angle of the chains.

## 4. Discussion

Our understanding of biological membranes remains incomplete and faces even greater enigmas when we consider what aspects of membrane physiology may be responsible for bacterial survival in diverse and particularly extreme environments. It is yet accepted that the inner membrane is central to microorganism survival, which are not insulated from extrinsic physical and chemical factors [27]. As a constant point of contact with the environment, flexibility in the adaptability of the cytoplasmic membrane and its components is a primary determinant of cell survival [27]. In a bacterial cytoplasmic membrane, limits of fluidity are generally defined by the thresholds beyond which the cell can no longer function. Physiological factors such as structurally unstable lipid bilayer or the inability to maintain membrane protein functions have been recognized as determinants of finite levels of membrane fluidity [27].

Whereas stimulating investigations were performed on changes of the whole proteome of fixed microorganisms as compared with that of planktonic counterparts [21], few were devoted to alterations in the membranal proteome and all focused on the outer membrane [28–30]. Surprisingly, very few took an interest in the inner membrane and/or in the membrane lipid profile [31].

*P. aeruginosa* membranes are known to contain usual lipid classes, i.e., PGs, PEs and DPGs, and unusual lipid classes such as PCs and LPGs [32]. This composition is different from that of *Escherichia coli* inner membrane which does not contain PCs. *P. aeruginosa* can synthesize PCs by methylation of PE using phospholipids methyltransferase [33]. In the present study, we mainly detected PEs and PGs. The most important alteration due to the growth mode (planktonic vs biofilm) was a drastic decrease of uneven-numbered chains in sessile bacteria as compared with planktonic counterparts. Another change was a slight statically relevant increase in PEs with long chains (PE 36 to PE 40).

Actually the uneven-numbered chains may either be branched chain phospholipids or cyclopropyl-containing chain phospholipids. In bacteria iso-C15, iso-C17, anteiso-C15 and anteiso-C17 saturated methyl-branched chain fatty acid are synthesized using leucine and isoleucine as substrates (the number is referring to the total number of carbons in the fatty acid chain) [34]. This is also the case for *P. aeruginosa* [35]. Bacteria also synthesize cyclopropane fatty acids (cyC) leading to cyclopropyl-containing chain phospholipids [36]. This is done by the addition of a

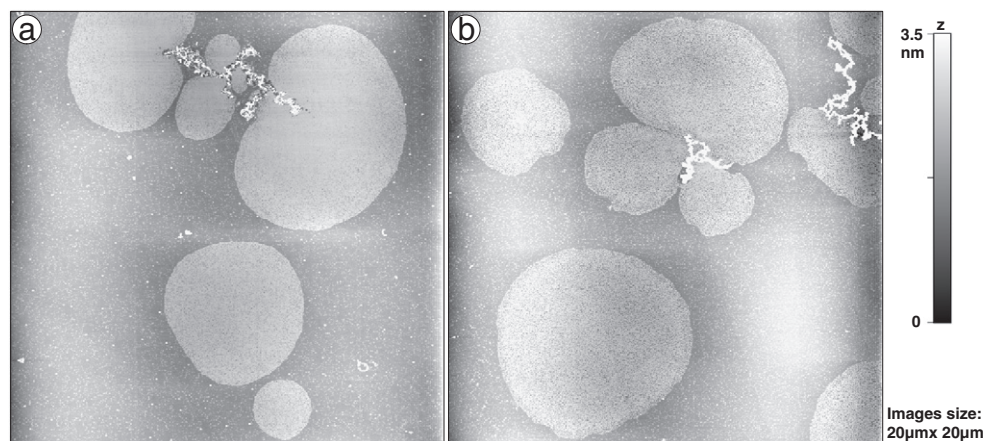


**Fig. 4.** Atomic Force Microscopy images of the transferred monolayers at 30 mN/m. Lipids were extracted from a) planktonic bacteria; b) sessile bacteria. Images were represented with a common z color scale (right bar). Condensed domains are higher than the surrounding expanded liquid phase and thus appear in light grey. Domains formed around aggregates are shown on the upper part of the images. Spontaneously formed domains of 6.4  $\mu\text{m}$  and 2.6  $\mu\text{m}$  diameters are shown on the left image (planktonic bacteria). On the right image (sessile bacteria) domains diameters are 9  $\mu\text{m}$  (bottom left) and 4.7  $\mu\text{m}$  (upper left).

methylene group from S-adenosyl-L-methionine to the cis double bond of an unsaturated fatty acid chain esterified to membrane phospholipid. Since the *cfa synthase* gene is present in *P. aeruginosa*, such phospholipids are also expected. In both cases this will lead to the detection of uneven-numbered chain phospholipids containing one chain with an uneven number of carbon. It should be noticed that cyclopropyl-containing chain phospholipids will be detected like phospholipids with one unsaturation (for example: PE 35:1 may likely be a phospholipid containing a) one iso- or anteiso-C17:0 and one C18:1 fatty acid chain, b) one C16:0 and one cyC19:0 or c) one C18:0 and one cyC17:0). Since saturated uneven-numbered phospholipids are detected, at least a part of the uneven-numbered phospholipids contain branched chains.

The role of cyclopropyl-containing chain phospholipids on the membrane properties is unclear especially concerning the modifications of membrane fluidity [36]. Branched chain phospholipids are known to be involved in the control of the membrane fluidity [37]. A decrease in branched chain phospholipids ratio in sessile bacteria would lead to a decrease in membrane fluidity. The presence of longer chains also suggests a better lipid stability in the bilayer and a decrease in membrane fluidity, confirming observations by Gianotti et al. [31]. Generally, acyl chain length increases bilayer stability with increasing carbon number longer chains penetrating deeper into the bilayer, increasing acyl chain interactions between layers and promoting a more rigid structure [38].

The slight increase of PEs with long chains and the decrease of uneven-numbered chains lipids may be related to cell adaptation to environmental conditions prevailing within biofilms. Indeed biofilms are characterized by the presence of detrimental conditions [39]. It has been shown that fatty acid composition of *P. aeruginosa* is largely modified by temperature and physiological state [40]. Alterations of the lipid composition in bacteria have been reported during the transition period from the late exponential phase to the stationary phase [41]. This seems to be a strategy to conserve energy by reducing membrane fluidity; bacteria in biofilms being less metabolically active than free-floating cells [1], adhered organisms might reduce membrane fluidity in order to conserve the energy.

Observations by Brewster Angle Microscopy and AFM showed that inner membrane lipids of *P. aeruginosa* could form domains when the surface pressure approached the pressure that exists in biological membranes. These domains were 50% larger when bacteria were grown as biofilms. This increase suggests either a higher proportion of saturated lipids, a higher proportion of lipids with long chains or a lower proportion of branched chain phospholipids in biofilm cells. Saturated or long chain lipids would lead to a higher condensing effect while unsaturated or uneven-numbered chain lipids would lead to a higher fluidity. Many previous works suggested the evidence of lipid membrane domains in both Gram positive and negative bacteria but their existence is still a hypothesis. It has been shown that inner membrane lipids of *E. coli* formed domains in model monolayers [26]. It should be noticed that the organisations of *E. coli* lipids in model monolayers are quite similar to those we observed here. Enrichment in cardiolipin was observed in *E. coli* using a specific marker of cardiolipin (NAO) at the septal of division and the poles of the plasma membrane [42]. A heterogeneous distribution of lipids and a selective staining of the septal region of division were also observed in *Mycobacterium* using a lipophilic fluorescent marker [43]. More recently, cardiolipin domains were also visualized with NAO in *P. putida* [44] confirming that lipid domains could exist in *Pseudomonas* genus. The larger domains which we observed for biofilm lipid extracts would lead to a decrease in the global membrane fluidity. This observation accords well with results obtained by ESI-MS which pointed out an increase in longer chain PEs and a decrease of branched chains. Branched chain lipids would be mainly present in the surrounding expanded liquid phase while long chains would be present in the condensed domains.

All these data demonstrate that the bacterial inner membrane lipidome is modified by the biofilm mode of growth. By such

metabolic adaptation, bacteria strive to maintain membrane order and viability face to changes in environmental and physicochemical conditions, e.g. pH, osmolarity, growth rate [45]. Maintenance of optimum membrane fluidity is crucial to healthy cell physiology, high fluidity being able to produce “leaky”, unstable membranes and low fluidity depriving inactive integral proteins of either their required lipid cofactors [46]. Such alterations of membrane protein activity might be involved in the low susceptibility of sessile organisms to some antibiotics, e.g., aminoglycosides whose uptake necessitates an active electron transport chain [47,48]. Recently, it was demonstrated that the composition, stability and lipid packing characteristics of the bacterial membrane play a role in the different fashions by which the VP1 antimicrobial peptide achieves its bactericidal effect on Gram positive and negative bacteria [49]. These physiological changes are under control of some transcription regulators. Thus, Des T was identified as a transcriptional regulator which controls the expression of genes involved in fatty acid biosynthesis in *P. aeruginosa* [50]. Des T senses the physical properties of the cellular acyl-CoA pool and modulates the expression of the acyl-CoA  $\Delta$  desaturase system to adjust fatty acid desaturation activity accordingly [51]. *P. aeruginosa* is also capable to regulate its fatty acid biosynthesis in response to changes in the growth conditions [52].

These phenotypic adaptations to the sessile mode of life reflect the bacterial ability to detect local cell density and thereby coordinate group behaviour [53]. It has been advanced that long chain fatty acids (LCFAs) may be environmental signals which affect through PsrA the transcription of *rpoS* and *exsC* genes. LCFAs increase N-(butyryl)-L-homoserin lactone quorum sensing (QS) signal and decrease the expression of ExoS/T [54]. Now, it is recognized that the QS is crucial for biofilm development [5]. All these data question about a correlation between lipid signals and the bacterial growth mode.

## 5. Conclusion

We showed here that the inner membrane lipidome was modified in *P. aeruginosa* sessile cells compared to free-floating counterparts. This modification is characterized by a drastic decrease of the uneven-numbered chain phospholipids and a relative accumulation of PEs with long chain lipids in biofilm organisms. Such alterations might play a key role in the particular physiology of biofilm cells. Consequently, bacterial fatty acid biosynthesis might be a new target for antibiofilm drug discovery [55].

## References

- [1] J.W. Costerton, P.S. Stewart, E.P. Greenberg, Bacterial biofilms: a common cause of persistent infections, *Science* 284 (1999) 1318–1322.
- [2] W.M. Dunne Jr., Bacterial adhesion: seen any good biofilms lately? *Clin. Microbiol. Rev.* 15 (2002) 155–166.
- [3] J.M. Schierholz, J. Beuth, G. Pulverer, Adherent bacteria and activity of antibiotics, *J. Antimicrob. Chemother.* 43 (1999) 158–160.
- [4] T.F. Mah, G.A. O'Toole, Mechanisms of biofilm resistance to antimicrobial agents, *Trends Microbiol.* 9 (2001) 34–39.
- [5] R.D. Monds, G.A. O'Toole, The developmental model of microbial biofilms: ten years of a paradigm up for review, *Trends Microbiol.* 17 (2009) 73–87.
- [6] P.S. Stewart, J.W. Costerton, Antibiotic resistance of bacteria in biofilms, *Lancet* 358 (2001) 135–138.
- [7] G. Stone, P. Wood, L. Dixon, M. Keyhan, A. Matin, Tetracycline rapidly reaches all the constituent cells of uropathogenic *Escherichia coli* biofilms, *Antimicrob. Agents Chemother.* 46 (2002) 2458–2461.
- [8] J. Zahler, P.S. Stewart, Transmission electron microscopic study of antibiotic action on *Klebsiella pneumoniae* biofilm, *Antimicrob. Agents Chemother.* 46 (2002) 2679–2683.
- [9] R.H.K. Eng, F.T. Padberg, S.M. Smith, E.N. Tan, C.E. Cherubin, Bactericidal effects of antibiotics on slowly growing and nongrowing bacteria, *Antimicrob. Agents Chemother.* 35 (1991) 1824–1828.
- [10] A. Ito, A. Taniuchi, T. May, K. Kawata, S. Okabe, Increased antibiotic resistance of *Escherichia coli* in mature biofilm, *Appl. Environ. Microbiol.* 75 (2009) 4093–4100.
- [11] E. Drenkard, F.M. Ausubel, *Pseudomonas* biofilm formation and antibiotic resistance are linked to phenotypic variation, *Nature* 416 (2002) 740–743.
- [12] C.Y. Loo, D.A. Corliss, N.J. Ganeshkumar, *Streptococcus gordonii* biofilm formation: identification of genes that code for biofilm phenotypes, *J. Bacteriol.* 182 (2000) 1374–1382.

- [13] C. Prigent-Combaret, O. Vidal, C. Dorel, P. Lejeune, Abiotic surface sensing and biofilm-dependent regulation of gene expression in *Escherichia coli*, *J. Bacteriol.* 181 (1999) 5993–6002.
- [14] C. Prigent-Combaret, E. Bombacher, O. Vidal, A. Ambert, P. Lejeune, P. Landini, C. Dorel, Complex regulatory network controls initial adhesion and biofilm formation in *Escherichia coli* via regulation of the *csgD* gene, *J. Bacteriol.* 183 (2001) 7213–7223.
- [15] M.A. Schembri, K. Kjærgaard, P. Klemm, Global gene expression in *Escherichia coli* biofilms, *Mol. Microbiol.* 48 (2003) 253–267.
- [16] M. Whiteley, M.G. Banger, R.E. Bumgarner, M.R. Parsek, G.M. Teitzel, S. Lory, E.P. Greenberg, Gene expression in *Pseudomonas aeruginosa* biofilm, *Nature* 413 (2001) 860–864.
- [17] M.C. Oosthuizen, B. Steyn, J. Theron, P. Cosette, D. Lindsay, A. Von Holy, V.S. Brozel, Proteomic analysis reveals differential protein expression by *Bacillus cereus* during biofilm formation, *Appl. Environ. Microbiol.* 68 (2002) 2770–2780.
- [18] K. Sauer, A.K. Camper, G.D. Ehrlich, J.W. Costerton, D.G. Davies, *Pseudomonas aeruginosa* displays multiple phenotypes during development as a biofilm, *J. Bacteriol.* 184 (2002) 1140–1154.
- [19] S. Vilain, P. Cosette, I. Zimmerlin, J.P. Dupont, G.-A. Junter, T. Jouenne, The biofilm proteome: homogeneity or versatility? *J. Prot. Res.* 3 (2004) 133–136.
- [20] S. Vilain, P. Cosette, M. Hubert, C. Lange, G.-A. Junter, T. Jouenne, Comparative proteomic analysis of planktonic and immobilized *Pseudomonas aeruginosa* cells: a multivariate statistical approach, *Anal. Biochem.* 329 (2004) 120–130.
- [21] G.-A. Junter, T. Jouenne, Immobilized viable microbial cells: from the process to the proteome... or the cart before the horse, *Biotechnol. Adv.* 22 (2004) 633–658.
- [22] B. Tummeler, U. Koopmann, D. Grothues, H. Weissbrodt, G. Steinkamp, H.V.D. Hardt, Nosocomial acquisition of *Pseudomonas aeruginosa* by cystic fibrosis patients, *J. Clin. Microbiol.* 29 (1991) 1265–1267.
- [23] T. Mizuno, M. Kageyama, Separation and characterization of the outer membrane of *Pseudomonas aeruginosa*, *J. Biochem.* 84 (1978) 179–191.
- [24] E.G. Bligh, W.J. Dyer, A rapid method of total lipid extraction and purification, *Can. J. Biochem. Physiol.* 37 (1959) 911–917.
- [25] S. Milne, P. Ivanova, J. Forrester, H.A. Brown, Lipidomics: an analysis of cellular lipids by ESI-MS, *Methods* 39 (2006) 92–103.
- [26] Z. Zerrouk, S. Alexandre, C. Lafontaine, V. Norris, J.-M. Valleton, Inner membrane lipids of *Escherichia coli* form domains, *Colloids Surf B* 63 (2008) 306–310.
- [27] N.C.S. Mykytczuk, J.T. Trevors, L.G. Leduc, G.G. Ferroni, Fluorescence polarization in studies of bacterial cytoplasmic membrane fluidity under environmental stresses, *Prog. Biophys. Mol. Biol.* 95 (2007) 60–82.
- [28] K. Otto, J. Norbeck, T. Larsson, K.A. Karlsson, M.J. Hermansson, Adhesion of type 1-fimbriated *Escherichia coli* to abiotic surfaces leads to altered composition of outer membrane proteins, *J. Bacteriol.* 183 (2001) 2445–2453.
- [29] D. Seyer, P. Cosette, A. Siroy, E. Dé, C. Lenz, H. Vaudry, L. Coquet, T. Jouenne, Proteomic comparison of outer membrane protein patterns of sessile and planktonic *Pseudomonas aeruginosa* cells, *Biofilms* 2 (2005) 27–36.
- [30] L. Coquet, P. Cosette, E. Dé, L. Galas, H. Vaudry, C. Rihouey, P. Lerouge, G.A. Junter, T. Jouenne, Immobilization induces alterations in the outer membrane protein pattern of *Yersinia ruckeri*, *J. Prot. Res.* 4 (2005) 1988–1998.
- [31] A. Gianotti, D. Serrazanetti, S.S. Kamdem, M.E. Guerzoni, Involvement of cell fatty acid composition and lipid metabolism in adhesion mechanism of *Listeria monocytogenes*, *Int. J. Food Microbiol.* 123 (2008) 9–17.
- [32] S.T. Albelo, C.E. Domenech, Carbons from choline present in the phospholipids of *Pseudomonas aeruginosa*, *FEMS Microbiol. Lett.* 156 (1997) 271–274.
- [33] P.J. Wilderman, A.I. Vasil, W.E. Martin, R.C. Murphy, M.L. Vasil, *Pseudomonas aeruginosa* synthesizes phosphatidylcholine by use of the phosphatidylcholine synthase pathway, *J. Bacteriol.* 184 (2002) 4792–4799.
- [34] T. Kaneda, Iso- and anteiso-fatty acids in bacteria: biosynthesis, function, and taxonomic significance, *Microbiol. Rev.* 55 (1991) 288–302.
- [35] V. Mc Cully, G. Burns, J.R. Sokatch, Resolution of branched-chain oxo acid dehydrogenase complex of *Pseudomonas aeruginosa* PAO, *Biochem. J.* 233 (1986) 737–742.
- [36] D.W. Grogan, J.E. Cronan JR, Cyclopropane ring formation in membrane lipids of bacteria, *Microbiol. Mol. Biol. Rev.* 61 (1997) 429–441.
- [37] M.C. Mansilla, L.E. Cybulski, D. Albanesi, D. de Mendoza, Control of lipid fluidity by thermal thermosensors, *J. Bacteriol.* 186 (2004) 6681–6688.
- [38] L. Rilfors, G. Lindblom, A. Wieslander, A. Christiansson, Lipid bilayer stability in biological membranes, in: M. Kates, L. Morris (Eds.), *Biomembranes*, vol. 12, Membrane Fluidity, Plenum Press, New York, 1984, pp. 206–245.
- [39] E. Karatan, P. Watnick, Signals, regulatory networks, and materials that build and break bacterial biofilms, *Microbiol. Mol. Biol. Rev.* 73 (2009) 310–347.
- [40] F.D. Brissonet, C. Malgrange, L. Guérin-Méchin, B. Heyd, J.Y. Leveau, Effect of temperature and physiological state on the fatty acid composition of *Pseudomonas aeruginosa*, *Int. J. Food Microbiol.* 55 (2000) 79–81.
- [41] J.T. Mac Garrity, J.B. Armstrong, The effect of salt on phospholipid fatty composition in *Escherichia coli* K-12, *Biochim. Biophys. Acta* 398 (1975) 258–264.
- [42] E. Mileykovskaya, W. Dowhan, Visualization of phospholipid domains in *Escherichia coli* by using the cardiolipin-specific fluorescent dye 10-N-nonyl acridine orange, *J. Bacteriol.* 182 (2000) 1172–1175.
- [43] H. Christensen, N.-J. Garton, R.W. Horobin, D.E. Minnikin, M.R. Barer, Lipid domains of *Mycobacteria* studied with fluorescent molecular probes, *Mol. Microbiol.* 1 (1999) 1561–1572.
- [44] P. Bernal, J. Munoz-Rojas, A. Hurtada, J.L. Ramos, A. Segura, A *Pseudomonas putida* cardiolipin synthesis mutant exhibits increased sensitivity to drugs related to transport functionality, *Environ. Microbiol.* 9 (2007) 1135–1145.
- [45] T.J. Denich, L.A. Beaudette, H. Lee, J.T. Trevors, Effect of selected environmental and physicochemical factors on bacterial cytoplasmic membranes, *J. Microbiol. Methods* 52 (2003) 149–182.
- [46] A.A. Herrero, R.F. Gomez, Development of ethanol tolerance in *Clostridium thermocellum*: effect of growth temperature, *Appl. Environ. Microbiol.* 40 (1980) 571–577.
- [47] R. Hancock, Uptake of <sup>14</sup>C streptomycin by some microorganisms and its relation to their streptomycin sensitivity, *J. Gen. Microbiol.* 28 (1962) 493–501.
- [48] O. Tresse, T. Jouenne, G.-A. Junter, The role of oxygen limitation in the resistance of agar-entrapped, sessile-like *Escherichia coli* to aminoglycoside and beta-lactam antibiotics, *J. Antimicrob. Chemother.* 36 (1995) 521–526.
- [49] S.R. Dennison, L.H.G. Morton, F. Harris, D.A. Phoenix, The impact of membrane lipid composition on antimicrobial function of an  $\alpha$ -helical peptide, *Chem. Phys. Lipids* 151 (2008) 92–102.
- [50] G.E. Schujman, D.D. Mendoza, Regulation of type II fatty acid synthase in Gram-positive bacteria, *Curr. Opin. Microbiol.* 11 (2008) 148–152.
- [51] Y.-M. Zhang, K. Zhu, M.W. Frank, C.O. Rock, A *Pseudomonas aeruginosa* transcription factor that senses fatty acid structure, *Mol. Microbiol.* 66 (2007) 622–632.
- [52] K.H. Choi, H.P. Schweizer, An improved method for rapid generation of unmarked *Pseudomonas aeruginosa* deletion mutants, *BMC Microbiol.* 5 (2005) 30.
- [53] B. Bassler, R. Losick, Bacterially speaking, *Cell* 125 (2006) 237–246.
- [54] Y. Kang, V.V. Lunin, T. Skarina, A. Savchenko, M.J. Schurr, T.T. Hoang, The long-chain fatty acid sensor, PrsA, modulates the expression of *rpoS* and the type III secretion *exsCEBA* operon in *Pseudomonas aeruginosa*, *Mol. Microbiol.* 73 (2009) 120–136.
- [55] D.J. Payne, P.V. Warren, D.J. Holmes, Y. Ji, J.T. Lonsdale, Bacterial fatty-acid biosynthesis: a genomic-driven target for antibacterial drug discovery, *Therapeutic Focus* 6 (2001) 537–544.